Novel Hybrid Monomers Bearing Cycloaliphatic Epoxy and 1-Propenyl Ether Groups

Surésh K. Rajaraman, William A. Mowers, and James V. Crivello*

Center for Polymer Synthesis, Department of Chemistry, Rensselaer Polytechnic Institute, Troy, New York 12180

Received July 9, 1998; Revised Manuscript Received October 23, 1998

ABSTRACT: The synthesis of a novel series of hybrid monomers containing cationically polymerizable cycloaliphatic epoxide and 1-propenyl ether functional groups in the same molecule has been conducted. Detailed structure−reactivity studies of the diaryliodonium salt-induced cationic photopolymerizations of these monomers indicate that the rate of epoxide ring-opening polymerization is markedly enhanced by the presence of the 1-propenyl ether group. At the same time, the polymerization of the 1-propenyl ether groups in such hybrid monomers is retarded. A mechanism involving the free-radical-induced decomposition of the photoinitiator has been proposed which serves to amplify the rate of the photoinitiated cationic epoxide ring-opening polymerization.

Introduction

In recent years, work in this laboratory has been directed toward the design of novel monomers specifically for use in photoinitiated cationic polymerizations.[1−4] Of particular interest are monomers that undergo very rapid photopolymerizations. These monomers have many potentially important uses in applications such as photocurable coatings, adhesives, and printing inks. Our initial work in this area focused on cycloaliphatic epoxides since these monomers undergo photoinitiated cationic polymerization at the highest rates of all known epoxides and also because the resulting polymers have excellent adhesion, chemical resistance, and mechanical properties.[5] For this reason, these monomers have become the mainstay of many industrial photocuring applications. Conversely, there is an increasing demand for epoxide monomers that undergo even more rapid photopolymerizations. Accordingly, we have undertaken a program to design and synthesize such monomers.

One recent approach we have taken for the design of new, more reactive epoxide monomers has been to incorporate other types of cationically polymerizable functional groups into these monomers. We call such monomers "hybrid" monomers. To enhance the reactivity of an epoxy monomer, it would appear reasonable to incorporate a functional group with an intrinsically higher reactivity. Previous studies from this group have shown that monomers containing the 1-propenyl ether group are among the most reactive functional groups known.[6] Their cationic polymerization rates exceed those of all epoxides, including the most reactive cycloaliphatic epoxides. Although hybrid monomers containing the glycidyl ether group and a 1-propenyl ether moiety in the same molecule have been synthesized,[7,8] there are no known examples of monomers containing both a cycloaliphatic epoxide and a 1-propenyl ether functional group.

The goal of the present investigation was to prepare such hybrid monomers and conduct a detailed investigation of their behavior in photoinitiated cationic polymerization. It was of special interest to determine whether the two types of functional groups would exhibit cooperative or differentiated reactivity during polymerization.

* To whom correspondence should be addressed.

Experimental Section

Materials and Characterization Techniques. All organic reagents employed in this investigation were reagent quality and were used as purchased from the Aldrich Chemical Co. (Milwaukee, WI) unless otherwise noted. 1,2,3,6-Tetrahydrobenzyl alcohol was purchased from Fluka-US (Milwaukee, WI) and was used as received. The photoinitiators (4-*n*-undecyloxyphenyl)phenyliodonium hexafluroantimonate (**IOC11**) and (4-*n*-decyloxyphenyl)phenyliodonium hexafluoroantimonate (**SOC10**) were prepared as described previously.[9,10]

^{1}H NMR spectra were obtained using Varian XL-200 and XL-500 spectrometers at room temperature in $CDCl_3$. All chemical shifts are reported relative to tetramethylsilane as an internal standard. Gas chromatographic (GC) analyses were performed on a Hewlett-Packard HP-5840A gas chromatograph equipped with a 15 m × 0.53 mm × 1.5 μm film thickness cross-linked methyl silicone gum column and a flame ionization detector. Differential scanning calorimetry (DSC) and thermogravimetric analysis (TGA) measurements were carried out under nitrogen and air at heating rates of 5 and 20 °C/min, respectively, using a Perkin-Elmer DSC-7 TGA-7 thermal analysis system. Elemental analyses were performed by Atlantic Microanalysis, Inc. (Norcross, GA).

Synthesis of Model Compounds and Monomers. A summary of the characteristics of the monomers and model compounds prepared in this study is presented in Table 1.

*Synthesis of (2-Oxapent-4-enyl)cyclohex-3-ene (**CA**). Method A.* Into a 500 mL round-bottom flask equipped with an overhead stirrer, a thermometer, and a nitrogen inlet were placed 56.085 g (0.5 mol) of distilled 1,2,3,6-tetrahydrobenzyl alcohol, 90.75 g (0.75 mol) of allyl bromide, 100 mL of toluene, and 30 g (0.75 mol) of sodium hydroxide. The reaction mixture was stirred at room temperature for 15 min. Then, 3 g (0.01 mol) of tetra-*n*-butylammonium bromide was added and the reaction mixture slowly heated to reflux (65 °C) and maintained at that temperature for 8 h. The reaction mixture was cooled and filtered to remove the sodium bromide that precipitated during the reaction. The filtrate was poured into 500 mL of distilled water, the organic layers were separated, and the aqueous layer was extracted with fresh toluene. The combined organic layers were washed with three 200 mL portions of distilled water, and the organic phase was dried over anhydrous sodium sulfate. Then, the excess allyl bromide

10.1021/ma981078r CCC: $18.00 © 1999 American Chemical Society
Published on Web 12/17/1998

Table 1. Characteristics of Hybrid Monomers and Model Compounds

			elemental analysis		
cmpd	bp (°C/mm)	yield (%)		% C	% H
CA	22/0.05	83	calc	78.90	10.59
			found	78.82	10.52
CP	156/20	92	calc	78.90	10.59
			found	78.79	10.53
CEA	30/0.1	69	calc	71.39	9.59
			found	71.36	9.55
CEP	165/22	93	calc	71.39	9.59
			found	71.39	9.53
MCA	28/0.1	89	calc	79.95	10.37
			found	79.90	10.32
MCP	130/25	95	calc	79.95	10.37
			found	79.83	10.28
MCEA	30/0.1	70	calc	72.89	9.45
			found	72.85	9.45
MCEP	142/25	94	calc	72.89	9.45
			found	72.82	9.39
NA	35/0.05	90	calc	80.44	9.82
			found	80.41	9.81
NP	172/25	94	calc	80.44	9.82
			found	80.42	9.77
NEA	40/0.05	60	calc	73.30	8.95
			found	73.19	8.91
NEP	160/15	94	calc	73.30	8.95
			found	73.08	8.88
MCPr	31/0.1	88	calc	78.58	11.98
			found	78.49	11.88
MCEPr	45/0.25	70	calc	71.70	10.94
			found	71.57	10.92

and toluene were removed using a rotary evaporator, and the reaction mixture was subjected to vacuum distillation. The clear liquid distillate amounted to 62.32 g (82% recovered yield). Fractional vacuum distillation gave pure **CA** with a boiling point of 22 °C at 0.05 mmHg.

^{1}H NMR ($CDCl_3$): δ (ppm) 1.1−1.4 (H_1, 1H); 1.5−2.3 ($H_2 + H_5 + H_6$, 6H); 3.15−3.5 (H_7, 2H); 3.8−4.1 (H_8, 2H); 5.1−5.4 (H_{10}, 2H); 5.5−5.8 ($H_3 + H_4$, 2H); 5.8−6.1 (H_9,1H).

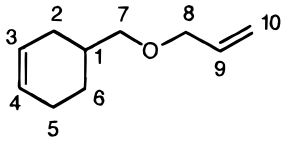

Elemental Analysis. Calculated for $C_{10}H_{16}O$: C, 78.90%; H, 10.59%. Found: C, 78.82%; H, 10.52%.

Method B. Into a 250 mL round-bottom flask equipped with a magnetic stirrer were placed 14.0 g (0.127 mol) of distilled 1,2,3,6-tetrahydrobenzaldehyde, 60 mL (0.869 mol) of allyl alcohol, and 16.24 g (0.14 mol) of triethylsilane. The reaction mixture was stirred at 0 °C for 1 h. Then, 25 mL of concentrated sulfuric acid was added dropwise over a period of 1 h using an addition funnel. The reaction mixture was slowly warmed to room temperature and maintained at that temperature for 1 h. To the above cooled reaction mixture was added 100 mL of pentane. This mixture was washed thrice with 100 mL of a saturated solution of sodium chloride. The organic layer was separated and dried over sodium sulfate. The excess allyl alcohol and pentane were removed using a rotary evaporator, and the reaction mixture was subjected to fractional vacuum distillation. The resulting clear liquid amounted to 12.8 g (73% recovered yield). Fractional distillation gave pure **CA** with a boiling point of 22 °C at 0.05 mmHg.

The ^{1}H NMR of the **CA** obtained by method B was similar to that obtained by method A.

Elemental Analysis. Calculated for $C_{10}H_{16}O$: C, 78.9%; H, 10.59%. Found: C, 78.79%; H, 10.57%.

*Synthesis of 1-(2-Oxapent-4-enyl)-6-methylcyclohex-3-ene (**MCA**).* A procedure analogous to that employed for **CA** (method A) was used to synthesize **MCA**. A yield of 89% was obtained. The compound had a boiling point of 28 °C at 0.1 mmHg.

^{1}H NMR ($CDCl_3$): δ (ppm) 0.7−1.1 ($H_1 + H_7$,4H); 1.5−2.4 ($H_2 + H_5 + H_6$, 6H); 3.2−3.6 (H_8, 2H); 3.8−4.1 (H_9, 2H); 5.1−5.4 (H_{11}, 2H); 5.5−5.75 ($H_3 + H_4$, 2H); 5.8−6.1 (H_{10},1H).

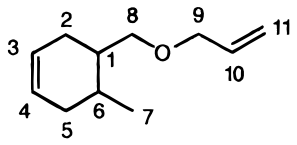

Elemental Analysis. Calculated for $C_{11}H_{17}O$: C, 79.95%; H, 10.37%. Found: C, 79.90%; H, 10.32%.

*Synthesis of (2-Oxapent-4-enyl)bicylo[2.2.1] hept-5-ene (**NA**).* **NA** was prepared using the same procedure employed for **CA** (method A). A yield of 90% was obtained. The compound had a boiling point of 35 °C at 0.05 mmHg.

^{1}H NMR ($CDCl_3$): δ (ppm) 0.3−0.5 (H_{6n}, 1H); 0.9−1.2 (H_{7anti}, 1H); 1.25−1.4 (H_{7syn}, 1H); 1.5−1.9 (H_{6x}, 1H); 2.1−2.4 (H_5, 1H); 2.6−3.5 ($H_1 + H_4 + H_8$, 4H); 3.8−4.1 (H_9, 2H); 5.0−5.4 (H_{11}, 2H); 5.8−6.0 (H_{10},1H); 6.0−6.3 ($H_2 + H_3$, 2H).

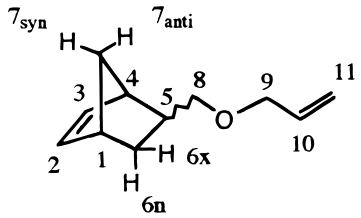

Elemental Analysis. Calculated for $C_{11}H_{16}O$: C, 80.44%; H, 9.82%. Found: C, 80.41%; H, 9.81%.

*Synthesis of (2-Oxapent-3-enyl)cyclohex-3-ene (**CP**).* To 19 g (0.125 mol) of **CA** in a 100 mL round-bottom flask equipped with a magnetic stirrer, reflux condenser, and a nitrogen inlet was added 0.008 g (0.0075 mmol) of tris(triphenylphosphine)-ruthenium(II) dichloride. The reaction mixture was heated at 160 °C for 2 h. The ^{1}H NMR spectrum showed that the bands assigned to the allyl groups (δ (ppm) 5.1−5.4, CH_2=; 5.8−6.1, CH=; 3.8−4.1, CH_2) had been completely replaced by new bands (δ (ppm) 1.58, CH_3; 4.25−4.45, *cis*-CH_3−C*H*=; 4.65−4.85, *trans*-CH_3−C*H*=; 5.9−6, *cis*-CH−O; 6.15−6.3, *trans*-O−CH) assigned to the 1-propenyl ether groups. Pure **CP** (mixture of *d,l-cis* and *d,l-trans* isomers) was isolated by fractional vacuum distillation (bp 156 °C at 20 mmHg) in 92% yield.

Elemental Analysis. Calculated for $C_{10}H_{16}O$: C, 78.9%; H, 10.59%. Found: C, 78.79%; H, 10.53%.

*Synthesis of (2-Oxapent-3-enyl)-6-methylcyclohex-3-ene (**MCP**).* The same procedure used for **CP** was used to synthesize **MCP**. A yield of 95% was obtained. The compound had a boiling point of 130 °C at 10 mmHg.

^{1}H NMR ($CDCl_3$): δ (ppm) 0.8−1 ($H_1 + H_7$,4H); 1.5−1.6 (H_{11}, 3H); 1.6−2.3 ($H_2 + H_5 + H_6$, 5H); 3.4−3.8 (H_8, 2H); 4.3−4.5 (H_{10z}); 4.7−4.9 (H_{10E}); 5.6−5.8 ($H_3 + H_4$, 2H); 5.9−6 (H_{9z}); 6.2−6.3 (H_{9E}).

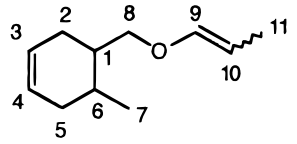

Elemental Analysis. Calculated for $C_{11}H_{17}O$: C, 79.95%; H, 10.37%. Found: C, 79.83%; H, 10.28%.

*Synthesis of (2-Oxapent-3-enyl)bicylo[2.2.1]hept-5-ene (**NP**).* A procedure analogous to **CP** was used to synthesize **NP**. Complete disappearance of the bands assigned to the allyl groups (δ (ppm) 5.0−5.4, CH_2=; 5.8−6.0, CH=; 3.7−4.0, CH_2) occurred only after 8 h of reaction. A yield of 94% of pure **NP**

(cis endo and exo isomers only) was obtained. **NP** had a boiling point of 172 °C at 25 mmHg.

^{1}H NMR ($CDCl_3$): δ (ppm) 0.3−0.5 (H_{6n}, 1H); 0.9−1.2 (H_{7anti}, 1H); 1.25−1.4 (H_{7syn}, 1H); 1.4−1.6 (H_{11}, 3H); 1.65−1.95 (H_{6x}, 1H); 2.2−2.5 (H_5, 1H); 2.7−3.5 ($H_1 + H_4 + H_8$, 4H); 4.3−4.5 (H_{10z}, 1H); 5.9−6.0 (H_{9E}, 1H); 6.0−6.3 ($H_2 + H_3$, 2H).

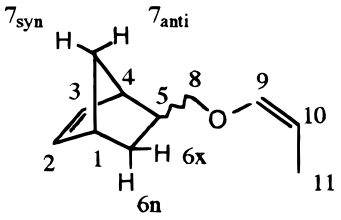

Elemental Analysis. Calculated for $C_{11}H_{16}O$: C, 80.44%; H, 9.82%. Found: C, 80.42%; H, 9.77%.

*Synthesis of (2-Oxapent-4-enyl)-3,4-epoxycyclohexane (**CEA**).* Into a 1 L round-bottom flask equipped with an overhead stirrer, an addition funnel, and a thermometer were placed 32.3 g of 3-chloroperoxybenzoic acid (0.1205 mol) and 300 mL of methylene chloride. The flask was cooled to 0−3 °C using an ice bath. **CA (**20 g, 0.1205 mol) in 150 mL of methylene chloride was added dropwise so that the temperature did not rise above 10 °C. The addition required approximately 90 min. The reaction was allowed to warm to room temperature, and then the mixture was stirred overnight. The reaction mixture was filtered using a Büchner funnel to remove 3-chlorobenzoic acid and the filtrate washed with 100 mL quantities of saturated sodium bicarbonate solution until the evolution of carbon dioxide ceased. The organic layer was dried over anhydrous sodium sulfate. Then, the excess methylene chloride was removed using a rotary evaporator and the reaction mixture subjected to vacuum distillation. The volatile clear liquid amounted to 13.96 g (69% recovered yield). Fractional distillation gave pure **CA** as a mixture of isomers with a boiling point of 30 °C at 0.1 mmHg.

^{1}H NMR ($CDCl_3$): δ (ppm) 0.8−1.35 (H_1, 1H); 1.35−2.3 ($H_2 + H_5 + H_6$, 6H); 3.0−3.5 ($H_7 + H_3 + H_4$, 4H); 3.8−4.1 (H_8, 2H); 5.0−5.4 (H_{10}, 2H); 5.7−6 (H_9,1H).

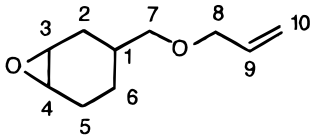

Elemental Analysis. Calculated for $C_{10}H_{16}O_2$: C, 71.39%; H, 9.59%. Found: C, 71.36%; H, 9.55%.

*Synthesis of (2-Oxapent-4-enyl)-6-methyl-3,4-epoxycyclohexane (**MCEA**).* An epoxidation procedure identical to that employed for **CEA** was used to synthesize **MCEA**. A yield of 70% was obtained. The mixture of isomers had a boiling point of 30 °C at 0.1 mmHg.

^{1}H NMR ($CDCl_3$): δ (ppm) 0.8−1.0 ($H_1 + H_7$, 4H); 1.35−2.3 ($H_2 + H_5 + H_6$, 5H); 3.0−3.5 ($H_3 + H_4 + H_8$, 4H); 3.8−4.1 (H_9, 2H); 5.0−5.4 (H_{11}, 2H); 5.7−6.05 (H_{10},1H).

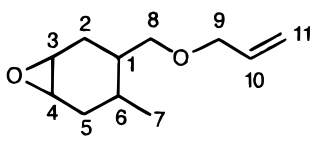

Elemental Analysis. Calculated for $C_{11}H_{17}O_2$: C, 72.89%; H, 9.45%. Found: C, 72.85%; H, 9.45%.

*Synthesis of (2-Oxapent-3-enyl)-3,4-epoxycyclohexane (**CEP**).* **CEA** was isomerized using a procedure identical to that used for **CP**. The isomerization reaction was complete after 9 h at 160 °C. A yield of 93% was obtained. **CEA** (mixture of eight isomers) had a boiling point of 165 °C at 22 mmHg.

^{1}H NMR ($CDCl_3$): δ (ppm) 0.9−1.35 (H_1,1H); 1.35−2.3 ($H_2 + H_5 + H_6 + H_{10}$, 9H); 3.1−3.3 ($H_3 + H_4$, 2H); 3.3−3.8 (H_7, 2H); 4.25−4.5 (H_{9z}); 4.65−4.95 (H_{9E}); 5.8−6.0 (H_{8z}); 6.1−6.3 ($H_{8E'}$).

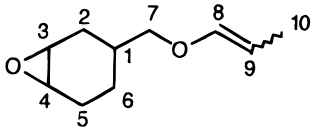

Elemental Analysis. Calculated for $C_{10}H_{16}O_2$: C, 71.39%; H, 9.59%. Found: C, 71.39%; H, 9.53%.

*Synthesis of (2-Oxapent-3-enyl)-6-methyl-3,4-epoxycyclohexane (**MCEP**).* An isomerization procedure analogous to **CP** was utilized for the synthesis of **MCEP**. The isomerization reaction was complete after 8 h at 160 °C. A yield of 94% of **MCEP** was obtained. The isomeric mixture had a boiling point of 142 °C at 15 mmHg.

^{1}H NMR ($CDCl_3$): δ (ppm) 0.7−1.05 ($H_1 + H_7$, 4H); 1.1−2.3 ($H_2 + H_5 + H_6 + H_{11}$, 8H); 3.0−3.3 ($H_3 + H_4$, 2H); 3.3−3.8 (H_8, 2H); 4.25−4.5 (H_{10z}); 4.7−4.9 (H_{10E}); 5.8−6.0 (H_{9z}); 6.1−6.3 ($H_{9E'}$).

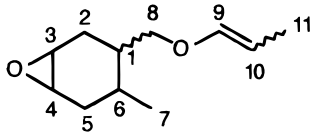

Elemental Analysis. Calculated for $C_{11}H_{17}O_2$: C, 72.89%; H, 9.45%. Found: C, 72.82%; H, 9.39%.

*Synthesis of (2-Oxapent-4-enyl)-3-oxatricylo[3.2.1.0^{2,3}]hept-5-ene (**NEA**).* Regioselective epoxidation of **NA** was conducted using a previously described procedure[2] to synthesize **NEA**. In a 3 L three-neck round-bottom flask equipped with a mechanical stirrer, two pressure equalizing addition funnels, and a thermometer were placed 20 g (0.1217 mol) of **NA**, 100 mL of acetone, 100 mL of dichloromethane, 500 mL of a phosphate buffer, and 0.5 g of 18-crown-6. The flask was cooled to 0 °C using an salt/ice/water bath, and 65 g of Oxone ($2KHSO_5$, K_2SO_4, $KHSO_4$) was added as a 0.4 M ice-cold, clear aqueous solution using one addition funnel. The pH of the solution was monitored using a narrow range pH (7.2−8.8) paper and was maintained at 7.4−7.6 using 1 N sodium hydroxide solution from the second addition funnel. After addition of Oxone solution was completed, the reaction was stirred at 5 °C for an additional 5−6 h. The product was filtered to remove precipitated solids, and the organic and aqueous layers were separated. The aqueous layer was extracted with four 100 mL quantities of dichloromethane, and the combined organic layers were washed with four 100 mL aliquots of distilled water. The organic layer was dried over anhydrous sodium sulfate, and the solvent was removed using a rotary evaporator. Distillation under reduced pressure gave **NEA** (60% yield) as a colorless liquid with a boiling point of 40 °C/0.05 mmHg.

^{1}H NMR ($CDCl_3$): δ (ppm) 0.5−0.85 (H_{6n}, 1H); 0.9−1.2 (H_{7anti}, 1H); 1.25−1.4 (H_{7syn}, 1H); 1.5−1.9 (H_{6x}, 1H); 2.1−2.4 (H_5, 1H); 2.4−2.6 ($H_1 + H_4$, 2H); 3.0−3.3 ($H_2 + H_3$, 2H); 3.3−3.5 (H_8, 2H); 3.8−4.1 (H_9, 2H); 5.0−5.4 (H_{11}, 2H); 5.8−6.1 (H_{10},-1H); 6.0−6.3 ($H_2 + H_3$, 2H).

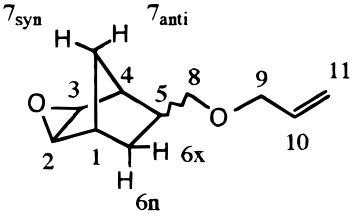

Elemental Analysis. Calculated for $C_{11}H_{16}O_2$: C, 73.30%; H, 8.95%. Found: C, 73.19%; H, 8.91%.

*Synthesis of (2-Oxa-pent-3-enyl)-3-oxatricylo[3.2.1.0^{2,3}]hept-5-ene (**NEP**).* A procedure analogous to that employed for **CP** was used to synthesize **NEP**. Complete disappearance of the bands assigned to the allyl groups (δ (ppm) 5.0−5.4, CH_2=; 5.8−6.1, CH=; 3.8−4.1, CH_2) occurred after 4 h. A yield of 94% of pure **NEP** (cis/trans ∼ 58:32) was obtained after purification by fractional vacuum distillation. The compound had a boiling point of 160 °C/15 mmHg.

^{1}H NMR ($CDCl_3$): δ (ppm) 0.7−0.9 (H_{6n}, 1H); 1.0−1.3 (H_{7anti}, 1H); 1.3−1.4 (H_{7syn}, 1H); 1.4−1.6 (H_{11}, 3H); 1.65−1.95 (H_{6x}, 1H); 2.2−2.4 (H_5, 1H); 2.4−2.6 (H_1 + H_4, 2H); 3.0−3.3 (H_2 + H_3, 2H); 3.4−3.8 (H_8, 4H); 4.3−4.5 (H_{10z}); 4.65−4.85 (H_{10E}); 5.8−6.0 (H_{9z}); 6.1−6.3 ($H_{9E'}$).

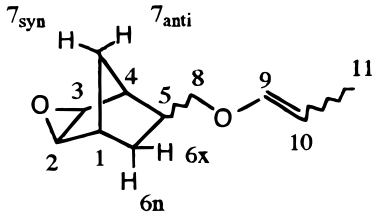

Elemental Analysis. Calculated for $C_{11}H_{16}O_2$: C, 73.30%; H, 8.95%. Found: C, 73.08%; H, 8.88%.

*Synthesis of 1-(2-Oxapentyl)-6-methylcyclohex-3-ene (**MCPr**).* A procedure analogous to **CA** (method A) was used to synthesize **MCPr**. A yield of 88% was obtained. The compound had a boiling point of 31 °C at 0.1 mmHg.

^{1}H NMR ($CDCl_3$): δ (ppm) 0.7−1.0 (H_{11} + H_7,6H); 1.5−1.9 (H_2 + H_5 + H_6, 6H); 1.9−2.3 (H_1 + H_{10}, 3H); 3.2−3.6 (H_8 + H_9, 4H); 5.5−5.8 (H_3 + H_4, 2H).

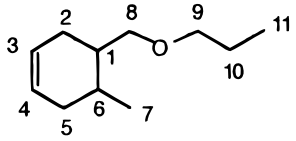

Elemental Analysis. Calculated for $C_{11}H_{20}O$: C, 78.58%; H, 11.98%. Found: C, 78.49%; H, 11.88%.

*Synthesis of 1-(2-Oxa-pentyl)-6-methyl-3,4-epoxycyclohexane (**MCEPr**).* An epoxidation procedure analogous to **CEA** was used to synthesize **MCEPr**. A yield of 70% was obtained. The compound had a boiling point of 45 °C at 0.25 mmHg.

^{1}H NMR ($CDCl_3$): δ (ppm) 0.7−1.0 (H_{11} + H_7,6H); 1.1−1.7 (H_2 + H_5 + H_6, 6H); 1.7−2.3 (H_1 + H_{10}, 3H); 3.0−3.2 (H_3 + H_4, 2H); 3.2−3.6 (H_8 + H_9, 4H).

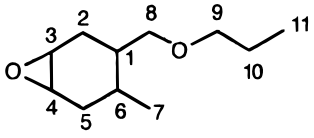

Elemental Analysis. Calculated for $C_{11}H_{20}O_2$: C, 71.7%; H, 10.94%. Found: C, 71.57%; H, 10.92%.

Polymerization Studies. Polymerizations of all the monomers were monitored using real-time infrared spectroscopy (RTIR). A Midac M-1300 FTIR spectrometer equipped with a liquid nitrogen cooled MCT detector was used. The instrument was fitted with a UVEXS model SCU-110 mercury arc lamp equipped with a flexible liquid optic wand. The end of this wand was placed at a distance of 5 cm and directed at an incident angle of 45° onto the sample window. The UV light intensity was measured with the aid of a International Light Co. Control-Cure radiometer at the sample window and was found to be 2200 mJ/cm^2 min (36.7 mW/cm^2).

Photopolymerizations were conducted at room temperature in bulk monomers containing 1 mol % **IOC11** or **SOC10** as the photoinitiator. **IOC11** was very soluble in **CEA**, **CEP**, **MCEA**, and **MCEP**. For **CP** and **MCP** the monomer/photoinitiator mixture was heated at 50 °C in a water bath for 10 min to achieve dissolution. The monomer/photoinitiator solutions were coated onto a 12 μm polypropylene film, covered with another polypropylene film, and then mounted in a 5 cm × 5 cm slide frame. Infrared spectra were collected at a rate of 0.5−3 spectra per second using a LabCalc, data acquisition software obtained from the Galactic Corp. and were processed using GRAMS-386 software from the same company. During irradiation, the decrease of the absorbance due to the 1-propenyl ether double bond centered at 1667 cm^{-1} and the decrease of the absorbance due to the epoxy group between 780 and 810 cm^{-1} were monitored. In all cases, experiments were performed in triplicate to verify reproducibility.

Results and Discussion

Synthesis of Monomers and Model Compounds. The syntheses of the desired hybrid monomers bearing cycloaliphatic epoxide groups together with 1-propenyl ether functionalities were carried out using simple, straightforward, and general reaction methods. Table 1 lists these compounds and summarizes their characterization data. As described in detail in the following sections, the overall synthesis involves three steps: (1) synthesis of an allyl ether of a cyclic alkene, (2) regioselective epoxidation of the cyclic alkene group, and finally (3) isomerization of the allyl ether to a 1-propenyl ether group to give the desired hybrid monomer. In addition, the preparations of several model compounds were also undertaken which were employed for mechanistic and kinetic studies.

It should be noted that the starting cyclic alkenols employed in the syntheses consisted of a mixture of stereoisomers. Hence, all the hybrid monomers were isolated as mixtures containing both stereoisomers and geometric isomers. No attempts were made to separate these complex mixtures into their individual pure isomeric components. Further, for brevity, the discussion will only refer to the geometric isomers due to the 1-propenyl ether double bond, although as noted in the structures shown, we acknowledge the presence of additional stereoisomers and geometric isomers as well.

*Synthesis of Allyl Ethers of Cyclic Alkenes **CA**, **MCA**, and **NA**.* The allyl ethers of three different cyclic alkenols were synthesized in high yields (82−90%) utilizing Williamson's ether synthesis. This reaction involves the nucleophilic displacement on allyl bromide with the sodium salt of the appropriate cyclic alkenol under phase-transfer conditions. This reaction (method A) is depicted in eq 1 for the synthesis of the allyl ether of 3-cyclohexene-1-methanol (1,2,3,6-tetrahydrobenzyl alcohol), **CA**.

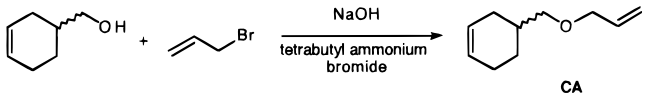

Using similar synthetic strategies, the allyl ethers of 6-methyl-3-cyclohexene-1-methanol (**MCA**) and 5-norbornene-2-methanol (**NA**) were also prepared.

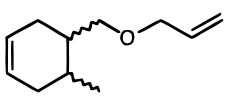

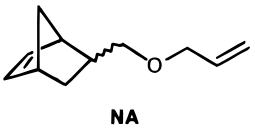

CA was also synthesized in good yield using a second method (method B)[11] which involves the acid-catalyzed reduction of 1,2,3,6-tetrahydrobenzaldehyde with triethylsilane in the presence of allyl alcohol to directly

afford the corresponding allyl ether. This reaction is depicted in eq 2.

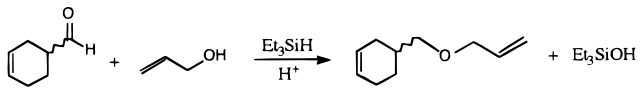

Method B described above utilizes as starting materials 1,2,3,6-tetrahydrobenzaldehyde and allyl alcohol which are respectively the precursors for 1,2,3,6-tetrahydrobenzyl alcohol and allyl bromide used in method A. For this reason and because of its simplicity, method B is potentially a highly attractive new synthetic route to **CA**, **MCA**, **NA**, and other related compounds.

*Synthesis of Model Compound 1-Propenyl Ethers **CP**, **MCP**, and **NP**.* The isomerizations of allyl ethers **CA**, **MCA**, and **NA** to their corresponding 1-propenyl ethers were conducted by treatment of the neat compounds at 160 °C with a catalytic amount of tris(triphenylphosphine)ruthenium(II) chloride. The preparations of these model compounds were undertaken for use in later photopolymerization studies. These reactions typically required 2 h for quantitative (92−95% isolated yield) isomerization to occur. The isomerization of **CA** is depicted in eq 3.

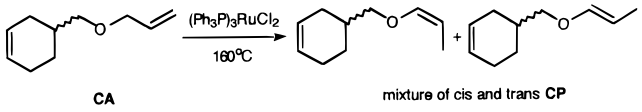

A mixture of cis and trans isomers was obtained. The cis-to-trans ratio was calculated using the integration of the ^{1}H NMR bands at 4.2−4.5 ppm (cis =C*H*−CH_3) and 4.7−4.9 ppm (trans =C*H*−CH_3) and was found to be 60/40.

Using analogous conditions, **MCA** and **NA** were isomerized to yield the corresponding 1-propenyl ethers, **MCP** and **NP**. The cis-to-trans ratio for **MCP** was found

to be 58/42. It is interesting to note that in previous studies[12] the ruthenium-catalyzed isomerization of allyl ethers usually gives a cis-to-trans ratio of isomers of 40/60 in favor of the trans isomer. In the case of **NP**, only the racemic cis isomers were isolated. When the isomerization reaction of **NA** was monitored using ^{1}H NMR spectroscopy, it was found that early in the reaction ($^1/_2$−1 h) both cis and trans **NP** isomers were formed. However, as the reaction proceeded further, the trans isomers disappeared, and only the racemic *cis*-1-propenyl ether was recovered. We suggest there is participation by both double bonds of these compounds as bidendate ligands in the coordination sphere of the ruthenium isomerization catalyst. In the specific case of **NA**, the coordination appears to be especially effective, resulting in the exclusive formation of the cis isomer. There are similar reports in the literature that describe the formation of the *cis*-1-propenyl isomer during the base-catalyzed isomerization of allyl ethers.[13,14] It is worth noting that no positional isomerization of the carbon−carbon double bond in the ring of either **CP** or **MCP** was observed under these reaction conditions.

*Regioselective Epoxidation of Allyl Ethers **CA**, **MCA**, and **NA**.* **CA**, **MCA**, and **NA** have two carbon−carbon double bonds in each of the molecules. We have utilized the higher reactivity of the cyclic alkene double bond to direct epoxidation regioselectively to this site. The epoxidations of **CA** and **MCA** were conducted under mild conditions using 1 equiv of 3-chloroperbenzoic acid. **NA** was epoxidized using dimethyldioxirane. Under both of these conditions, only the cycloaliphatic double bonds epoxidized, leaving the allylic double bonds unaffected and giving the desired epoxy allyl ethers in good yields. This reaction is depicted in eq 4 for the epoxidation of **CA**.

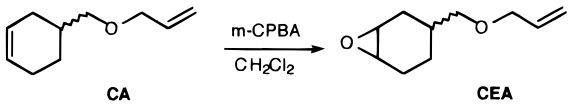

Similarly, the epoxidation of **MCA** was carried out using identical conditions to give **MCEA**. **NA** could not

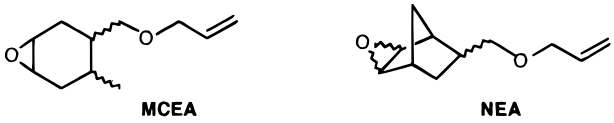

be successfully epoxidized using 3-chloroperbenzoic acid due to ring-opening side reactions. Instead, dimethyldioxirane generated by the reaction of potassium peroxysulfate (Oxone) and acetone was used. The yield (unoptimized) obtained was ∼70%.

Isomerization of Epoxy Functionalized Allyl Ethers. The isomerizations of epoxy functionalized allyl ethers **CEA**, **MCEA**, and **NEA** were carried out in a manner similar to that described previously for the isomerizations of model compound allyl ethers **CA**, **MCA**, and **NA** using tris(triphenylphosphine)ruthenium(II) chloride as a catalyst. The reactions proceeded to afford the desired epoxy functionalized 1-propenyl ethers (hybrid monomers) in high yields (∼94%). The cis-to-trans ratios for the isomerizations of **CEA** and **MCEA** were approximately 60/40. The structures of the compounds obtained are depicted below.

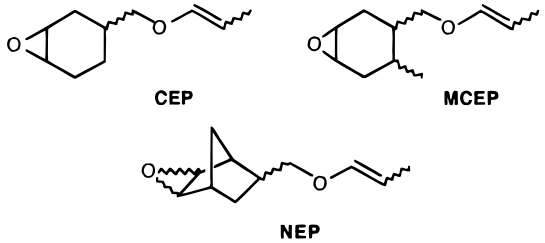

It was observed that the double-bond isomerization of the epoxy functionalized allyl ethers took place considerably more slowly than that of simple allyl ethers. Whereas model compound allyl ethers **CA** and **MCA** undergo the isomerization in less than 2 h, the complete isomerization of epoxy functionalized allyl ethers required 8 h. One possible explanation for the slower reaction rate is the competitive complexation between both the epoxy and the allyl groups with catalytically active ruthenium species during the isomerization reaction.

No attempt was made to carry out the epoxidation of cycloaliphatic 1-propenyl ethers (such as **CP**, **MCP**, or **NP**) as a route for the synthesis of epoxy functional

1-propenyl ether hybrid monomers **CEP**, **MCEP**, and **NEP**. This is due to the sensitivity of the 1-propenyl ether functional group to hydrolysis under the acidic conditions typically used for epoxidations.

Photoinitiated Cationic Polymerization of Hybrid Monomers. The cationic polymerizations of the hybrid monomers prepared as described in this paper containing two highly reactive cationically polymerizable groups are inherently difficult to follow by conventional methods. This is not only due to the fact that the polymerizations are exceedingly rapid, but also because the polymers that are formed are cross-linked. When typical initiators such as Lewis and Brønsted acids are added to these monomers, gel formation sets in even before the catalysts can be homogeneously dispersed in the reaction mixture. The above difficulties can be offset through the use of latent onium salt photoinitiators such as diaryliodonium salts. Polymerizations can be induced on demand through the irradiation of the monomer−photoinitiator mixtures with ultraviolet light. Throughout the course of this investigation, we used (4-*n*-undecyloxyphenyl)phenyliodonium hexafluroantimonate (**IOC11**) as the photoinitiator. **IOC11** has been delib-

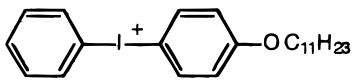

IOC11

erately designed for maximum solubility in a wide variety of polar and nonpolar monomers. The enhanced solubility is provided both by the unsymmetrical structure of the photoinitiator and by the long alkoxy chains containing an odd number of carbon atoms. UV irradiation at the λ_{max} (247 nm) of this salt results in facile photolytic decomposition with a high quantum yield ($\phi = \sim 0.7$). The overall mechanism of photolysis is shown in eqs 5−7.[15−17] UV irradiation and absorption of light results in both homolytic and heterolytic cleavage of a carbon−iodine bond of the diaryliodonium salt (eq 5).

$$\mathrm{Ar_2I^+X^-} \xrightarrow{h\nu} \mathrm{ArI^{\bullet +}X^-} + \mathrm{Ar^\bullet} \xrightarrow{h\nu} \mathrm{ArI} + \mathrm{Ar^+X^-} \quad (5)$$

The products of the photolysis are cationic and cation radical species that further react to form a strong protonic acid (eq 6). In the case of **IOC 11**, $HSbF_6$ is formed, which is the strongest acid known.

$$\mathrm{ArI^{\bullet +}X^-} + \mathrm{Ar^\bullet} \xrightarrow{\mathrm{RH}} \mathrm{HX} + \text{products}$$
$$\mathrm{ArI} + \mathrm{Ar^+X^-} \xrightarrow{\mathrm{RH}} \mathrm{HX} + \text{products} \quad (6)$$

This strong protonic acid is the primary species responsible for initiation of cationic polymerization (eq 7). Both the initiation and the propagation (eq 8) steps are dark reactions (i.e., nonphotochemical processes).

$$\mathrm{HX} + \mathrm{M} \rightarrow \mathrm{HM^+X^-} \quad (7)$$

$$\mathrm{HM^+X^-} + n\mathrm{M} \rightarrow H(M)_{n-1}\mathrm{M^+X^-} \quad (8)$$

The cationic photopolymerization of the monomers synthesized during this investigation were studied using a simple but powerful technique called Fourier transform real-time infrared spectroscopy (RTIR). This technique involves monitoring the decrease of characteristic absorption of a functional group undergoing polymerization as a function of time.[18] Since the integrated areas of the above-mentioned absorptions are directly proportional to the conversions at any given time, one directly obtains plots of the reaction profiles. Since the initial slopes of these curves are proportional to the rates of polymerization, the extents of reaction can be calculated from these data. Typically, the conversions increase with time until a maximum value referred to as the limiting conversion is reached.

Since the RTIR monitors the change in intensity of the bands of a characteristic functional group participating in polymerization, the first step was to identify the appropriate bands for each monomer. The asymmetric stretching bands due to the epoxy bonds appear at 740−850 cm^{-1}. The carbon−carbon double-bond stretching vibrations are centered at 1673 cm^{-1}. The above band regions were chosen because they were the ones least obscured by other bands in the spectra. It is important to note that in these studies we refer to band regions rather than a single band. This, as noted before, is because the monomers used in this study are not isomerically pure. Rather, they consist of a mixture of geometrical and stereochemical isomers. For example, monomer **MCEP** contains two chiral centers as well as two sites of geometrical isomerism (the epoxide and double bond) which give rise to a total of 16 possible isomers. The presence of these isomers leads to different vibrational frequencies and, consequently, different IR absorptions for the same two functional groups. Further, the various isomers would be expected to exhibit different propensities toward polymerization since they possess both uniquely different thermodynamic and steric characteristics. In this study, we monitored the reactivity of all the various isomers present in the mixture simultaneously. As a result, the photopolymerizations reported here are, in fact, copolymerizations of closely related monomeric species. In this work, the assumption was made that the IR absorption coefficients of the epoxide and 1-propenyl ether groups of the various isomers were the same. Based on this assumption, the integrated intensities were summed for the isomeric mixtures, and the overall conversions were calculated.

Previous studies of the cationic photopolymerization of hybrid monomers such as glycidyl 1-propenyl ether revealed some very interesting characteristics of this class of monomers.[8] First, due to the proximity of the two functional groups in the molecule, considerable intramolecular cyclization was observed. In the present monomers, the distance between the two disparate functional groups is greater, and we expected that less intramolecular cyclization would result in these molecules. Second, observation of the individual rates of consumption of the epoxy and 1-propenyl groups in glycidyl 1-propenyl ether showed that the rate of polymerization of the epoxide group was higher than that of the 1-propenyl ether group. Thus, despite the much greater reactivity in the cationic polymerization of simple 1-propenyl ethers as compared to the glycidyl ether containing monomers, faster polymerization of the less reactive group in the hybrid monomer was noted. This phenomenon was ascribed to the ability of carbocations generated from the 1-propenyl ether monomer to rapidly cross over to the oxonium ions by attack of

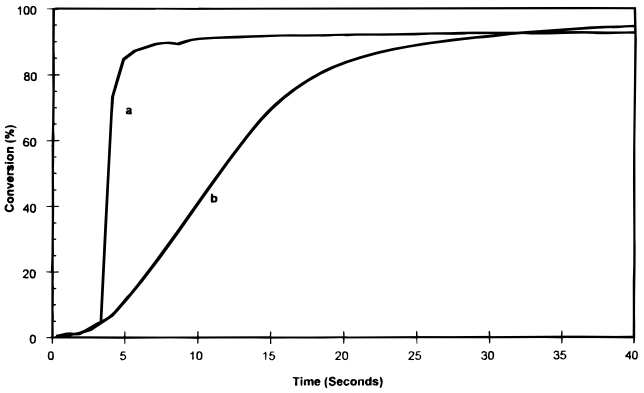

Figure 1. Study of the independent photoinitiated cationic photopolymerizations of **CP** (a) (1-propenyl ether) and **CEA** (b) (epoxide).

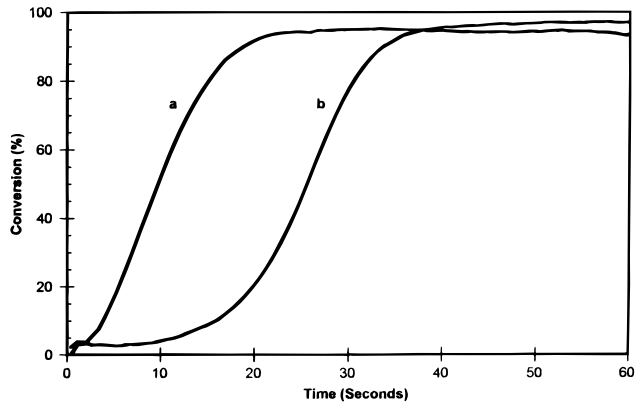

Figure 2. Study of the photoinitiated cationic polymerizations of a 1:1 mixture of **CP** (b) (1-propenyl ether) and **CEA** (a) (epoxide).

an epoxy monomer. The opposite crossover reaction, i.e., conversion of an oxonium ion chain end to a carbenium ion, either does not occur or takes place slowly.

The cycloaliphatic epoxide groups in the present monomers are considerably more reactive than the glycidyl ether groups in the previous monomers. As a result, the reactivity of these groups more closely match that of the 1-propenyl ether moieties in the same molecule. For this reason, it was of interest to determine which group in the hybrid monomer would exhibit the higher reactivity and also whether appreciable intramolecular cyclization takes place.

Photopolymerizations of ***CP***, ***CEA***, *and* ***CEP.*** The RTIR conversion versus time curves for the independent photoinitiated cationic polymerizations of the epoxy monomer **CEA** and 1-propenyl ether monomer **CP** are shown in Figure 1. As in all the studies reported in this paper, each kinetic run was carried out at 25 °C in triplicate, and the resulting conversion versus time curves show a reproducibility of ±5%. A comparison of the two curves shows that the polymerizations of both epoxy and 1-propenyl ether functional groups of these two monomers proceed to very high conversions. However, as expected, the polymerization of the 1-propenyl ether group is considerably faster than that of the epoxy group.

In a second study depicted in Figure 2 is shown the simultaneous polymerization of a 1:1 molar mixture of the model compounds **CEA** and **CP**. In contrast to the previous results, the polymerizations of the epoxide and the 1-propenyl ether groups in the mixture take place a nearly the same rates as indicated by the slopes of

Scheme 1

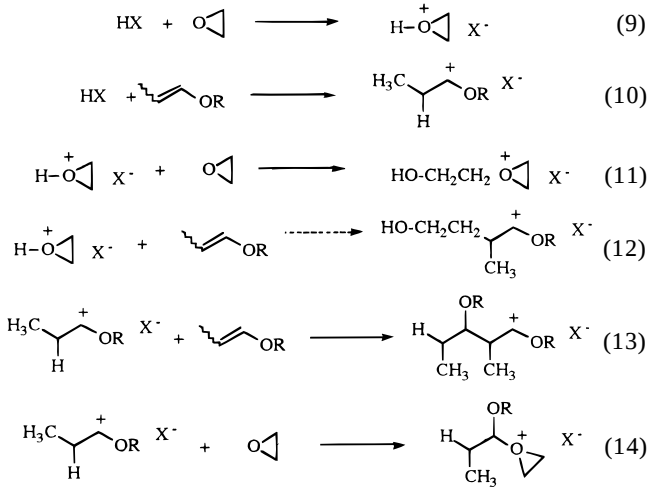

the curves. Both polymerizations proceed to very high (>95%) conversions. However, it may also be noted that, first, surprisingly the polymerization of the epoxycyclohexyl groups proceeds faster than that of the 1-propenyl ether groups and, second, the polymerization of these latter groups is effectively suppressed until the consumption of the epoxide groups is virtually complete. It may also be observed by comparison with Figure 1 that the rate of polymerization of the epoxy group of **CEA** in the mixture is accelerated in the presence of the 1-propenyl ether.

Previously,[19] we had reported that the monomer 1-butenyl glycidyl ether containing both enol ether and epoxy groups exhibited an acceleration of the rate of polymerization of the epoxide group. We attributed this effect to the ability of that monomer to undergo intramolecular cyclization reactions involving the two reactive groups. However, since the rate acceleration effect is also observed for a 1:1 mixture of **CEA** and **CP** in which only intermolecular interactions are possible, another explanation must be considered and will be discussed later.

The observation that the ring-opening polymerization of **CEA** precedes that of **CP** can be explained by considering the mechanism shown in Scheme 1. As noted earlier, photolysis of the diaryliodonium salt photoinitiator (eqs 5 and 6) results in the generation of a number of reactive species including aryl radicals, aryl cation radicals, aryl cations, and the superacid $HSbF_6$. Initiation of cationic polymerization can occur by protonation or attack of aryl cations on either the epoxide (eq 9) or 1-propenyl ether (eq 10). In eqs 9 and 10 only the attack by protons is shown, since these are overwhelmingly the most prominent species involved in initiation. While cationic polymerization of the protonated epoxide (oxiranium ion) can take place by nucleophilic attack of another epoxide group (eq 11), attack by a 1-propenyl ether group (eq 12) either does not occur or takes place very slowly due to the relatively high stability of the oxiranium ion as compared to that of the carbocation which is formed. Similarly, the carbocation which is formed by the initial protonation of the 1-propenyl ether groups can induce polymerization of either another 1-propenyl ether or an epoxide group (eqs 13 and 14). Using the same rationale, the crossover reaction (eq 14) would be expected to take place rapidly to convert the carbocation to the more stable oxonium ion.

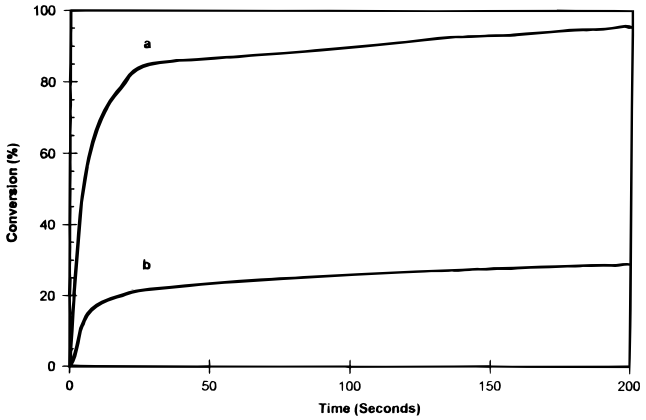

Figure 3. RTIR study of the photoinitiated cationic polymerization of **CEP** in the presence of 1 mol % **IOC-11**: (a) epoxide; (b) 1-propenyl ether.

The RTIR conversion versus time curves for the photoinitiated cationic polymerization of the epoxy and 1-propenyl ether groups of the hybrid monomer **CEP** are shown in Figure 3. Inspection of the curves shows that the polymerizations of the epoxycyclohexyl groups are very rapid and that these moieties undergo a more rapid reaction than the 1-propenyl ether groups. In addition, the conversion of the of the epoxy functional groups reaches 95%, while in the case of the 1-propenyl ether groups, the ultimate conversion is only about 35%. Therefore, it appears that the epoxide polymerization undergoes a dramatic acceleration due to the presence of the 1-propenyl ether group in the same molecule. The acceleration effect of the epoxide polymerization in **CEP** is even more pronounced than in the 1:1 molar mixture of model compounds **CEA** and **CP**. We have ascribed this incremental acceleration effect to an intramolecular interaction between the epoxide and propenyl ether groups.

Since, as noted above, rapid crossover from 1-propenyl ether to epoxide takes place while the reverse cross propagation reaction either occurs slowly or does not take place, ring-opening homopolymerization of the epoxide proceeds until virtually all these functional groups are exhausted. When this occurs, 1-propenyl ether polymerization rapidly sets in. These two separate stages of the polymerization have a direct impact on the structure of the polymer which is formed from **CEP**. This is depicted in eq 15.

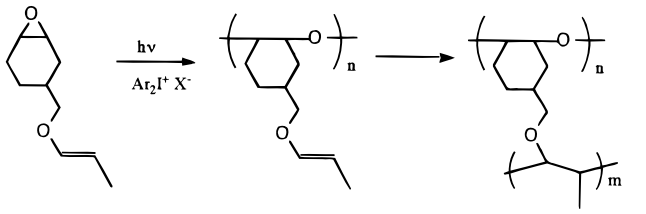

(15)

In the first stage, the polymer formed is substantially a linear polyether bearing pendant 1-propenyl ether groups. In the second, this polymer undergoes cross-linking by reaction of the pendant groups. Thus, the epoxide polymerization proceeds to very high conversions since a linear, soluble polymer is produced. However, while the initial stages of the 1-propenyl ether polymerization proceeds at a high rate, the polymerization slows and stops as the density of the cross-linked network increases and the glass transition temperature rises. Due to the immobility of the remaining 1-propenyl ether groups, an ultimate conversion of only 35% is attained.

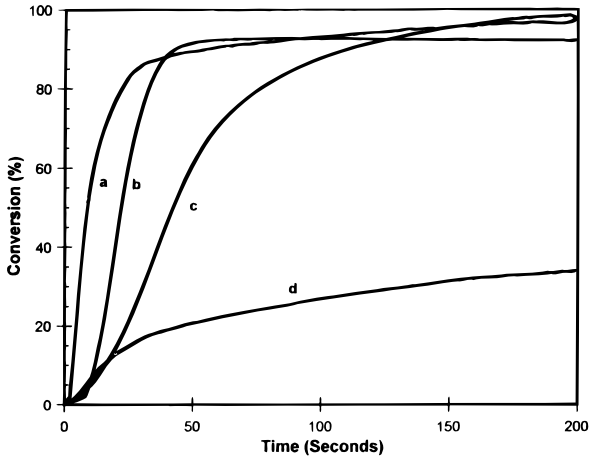

Figure 4. RTIR comparison of the photoinitiated cationic polymerizations of **MCP** (b) (1-propenyl ether), and **MCEA** (c)-(epoxide), **MCEP** (a) (epoxide), and **MCEP** (d) (1-propenyl ether).

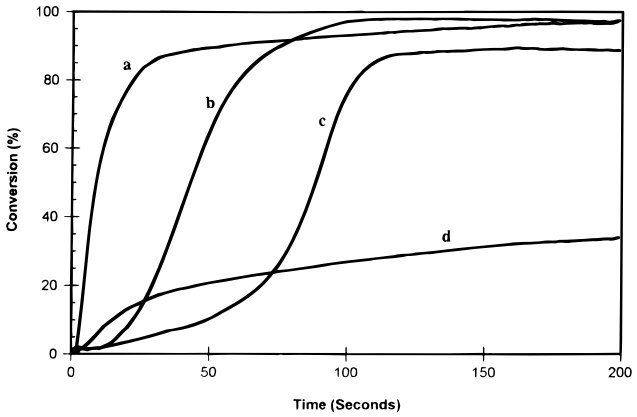

Figure 5. RTIR comparison of the photoinitiated cationic polymerization of a 1:1 mixture of **MCP** (b) (1-propenyl ether)- and **MCEA** (c) (epoxide) and of **MCEP** (a) epoxide and **MCEP** (d) (1-propenyl ether).

We have also noted that the apparent rate acceleration of an epoxide polymerization in the presence of a 1-propenyl ether is a general phenomenon and can be observed for many other combinations of these two types of monomers. Studies that document this phenomenon will be presented in later communications.

*Photopolymerizations of **MCP**, **MCEA**, and **MCEP**.* Identical observations were made for the photoinitiated cationic polymerization of **MCEP** as were found for **CEP**. In Figure 4 is depicted the RTIR curves obtained for the polymerization of the epoxide and 1-propenyl ether groups in this hybrid monomer. These curves are presented for comparison in the same figure together with the individual model compound polymerizations of the epoxide groups in **MCEA** and the 1-propenyl ether groups in **MCP**. Again, a marked acceleration of the polymerization of the epoxycyclohexyl groups and a deceleration of the 1-propenyl ether moieties of **MCEP** take place. In effect, the reactivity of the epoxide group in **MCEP** resembles that of an independent 1-propenyl ether group. It may also be noted that not only is the rate of the 1-propenyl ether polymerization suppressed but also so is the conversion. Figure 5 presents the curves obtained when the photopolymerizations of **MCEA**

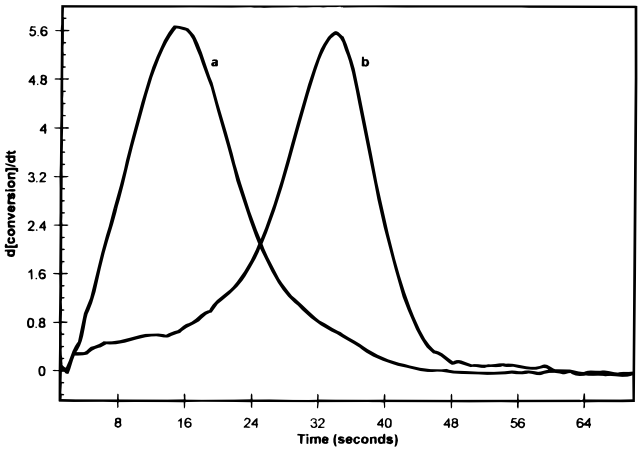

Figure 6. Derivative plots of the RTIR curves for (a) the epoxy polymerization of **MCEA** and (b) the 1-propenyl ether polymerization of **MCP**.

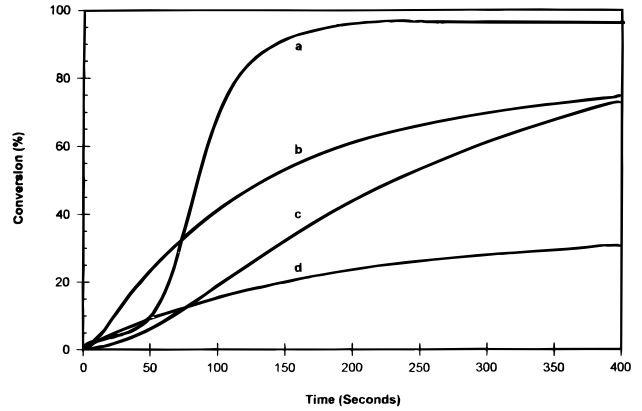

Figure 7. RTIR study of the polymerizations of **NEP** (b) (epoxide), (d) (1-propenyl ether); **NP** (a) (1-propenyl ether); **NEA** (c) (epoxide).

and **MCP** are carried out in a 1:1 molar mixture. The curves for the polymerization of **MCEP** are again superimposed on these two latter curves for comparison. When the equimolar mixture of **MCEA** and **MCP** is polymerized, the rate of the epoxide monomer polymerization is accelerated and the 1-propenyl ether monomer is depressed. Comparison of these model compound polymerizations with **MCEP** again indicates that the rate of the epoxide polymerization in **MCEP** is unexpectedly high. It is also worth noting that, again, the polymerization of the epoxide group of **MCEA** is nearly complete before the onset of the **MCP** 1-propenyl ether polymerization. This can be most easily seen in Figure 6 in which the corresponding curves in Figure 5 are plotted as their derivatives. It is clear from Figure 6 that the two polymerizations occur sequentially rather than simultaneously. To account for these results, it must be concluded from the study of this monomer as well as that of **CEP** that there must be an appreciable amount of intramolecular reaction between the two different functional groups in the same molecule which gives rise to a very rapid crossover reaction from 1-propenyl ether polymerization to ring-opening epoxide polymerization.

Photopolymerizations of ***NP***, ***NEA***, *and* ***NEP.*** Shown in Figure 7 are a series of RTIR curves for the photopolymerization of the hybrid epoxy 1-propenyl ether monomer **NEP** and several related model compounds. The photoinitiated cationic ring-opening epoxide polymerization of **NEP** is slower than that of either **CEP** or **MCEP**; however, like these latter two monomers it is more rapid than the 1-propenyl ether group in the same molecule. The comparatively slow epoxide polymerization of **NEP** is due to the steric hindrance provided by the bicyclic norbornenyl ring, and this effect has been observed previously.[20] Also shown for comparison in Figure 7 are the epoxide polymerizations of the epoxide group of the isomeric allyl ether compound and precursor **NEA** as well as the 1-propenyl ether **NP**. Very rapid polymerization of the sterically hindered 1-propenyl ether of **NP** takes place while polymerization of the epoxide group of **NEA** is slower than that of **NEP**.

Scheme 2

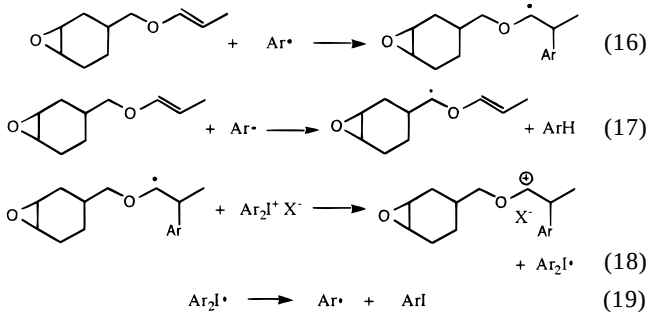

The outstanding reactivities of hybrid monomers **CEP** and **MCEP** were further demonstrated in a practical manner by spreading them as thin films containing 0.5 mol % **IOC11** onto a steel substrate and then irradiating them in a 300 W Fusion Systems Laboratory UV cure system. Using this apparatus, equipped with a conveyor, the speed with which cross-linking takes place can be estimated. Both **CEP** and **MCEP** were fully cross-linked at the highest speed of the conveyor (46 m/min, 150 ft/min) while **NEP** required two exposures at this speed for conversion to a tack-free film.

Mechanistic Studies. While the above mechanistic concepts explain why the ring-opening polymerizations of epoxide groups in the hybrid monomers take place before that of the 1-propenyl ether groups, they do not offer an adequate rationale for the apparent acceleration of the epoxide group polymerization of these monomers. Shown in Scheme 2 is a mechanism that we propose to explain this latter phenomenon.

As noted previously in eq 5, the photolysis of diaryliodonium salts generates not only cationic species (protons and cation radicals) but also free-radical species as well. Aryl radicals can interact with hybrid monomers such as **CEP** via the two pathways shown in eqs 16 and 17. A secondary radical species is generated by addition of the radical to the propenyl ether double bond (eq 16) or by abstraction of one of the labile hydrogen atoms adjacent to the ether oxygen (eq 17). Of these two reactions, addition of a free radical to the double bond (eq 16) appears to be the dominant process responsible for the acceleration effects in hybrid monomers. Redox interaction of either of the resulting radical species with the diaryliodonium salt gives rise to a carbocation and a diaryliodine radical. Only one of these reactions is depicted in eq 18. In a subsequent reaction (eq 19) the diaryliodine radical decays irreversibly to afford an aryl iodide and to regenerate the aryl free radical. The reactions shown in eqs 16−19 constitute a free-radical chain reaction in which the diaryliodonium salt is consumed by a nonphotochemical process. In addition, carbocations are generated that subsequently initiate

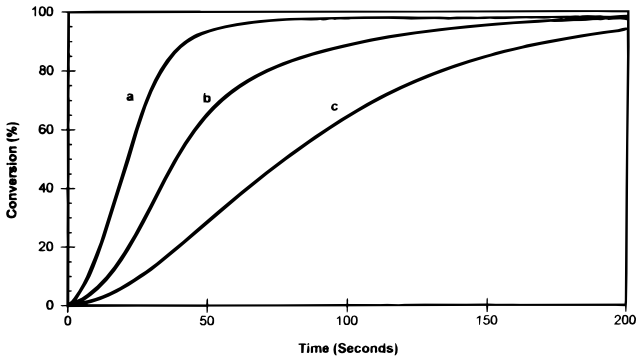

Figure 8. Comparison of the epoxide ring-opening photopolymerization of **MCEP** (a) alone, (b) in the presence of 4% nitrobenzene as a free-radical retarder, and (c) using **SOC10** as photoinitiator.

cationic polymerization. Initiation can occur by both an inter- and intramolecular process. Modeling studies suggest that the cation shown in eq 18 can attack the epoxide oxygen in the same molecule via a strain-free seven-membered-ring intermediate. This process may account for the higher rates of epoxide polymerization of the hybrid monomers as compared to 1:1 mixtures of propenyl ether and epoxide monomers. A similar mechanism involving free-radical addition, oxidation, and intermolecular attack can also be written to explain the rate acceleration effects observed in those cases in which equimolar amounts of propenyl ether and epoxide monomers are simultaneously polymerized. Consideration of Scheme 2 leads to the overall conclusion that the photochemically induced decomposition of the diaryliodonium salt photoinitiator is greatly amplified by the redox cycle of eqs 16−19. This results in a very rapid and efficient generation of a large number of initiating species, resulting in the observed high apparent rate of consumption of the epoxide groups.

There is some precedent for the mechanism shown in Scheme 2. We have previously reported that the photoinitiated cationic polymerization of 1-propenyl ether monomers is accelerated by a very similar mechanism involving a free-radical-induced decomposition of the photoinitiator.[21] In addition, we have also proposed that the electron-beam-induced cationic polymerization of epoxy monomers occurs by such a process.[22] To obtain some evidence for involvement of this mechanism with the present monomer, the photoinitiated cationic polymerization of **MCEP** was carried out in the presence of nitrobenzene as a free-radical retarder. The results are shown in Figure 8 which shows only the curves for disappearance of the 740−850 cm^{-1} epoxy bands. When the free-radical-induced decomposition reaction is retarded by nitrobenzene, the epoxide polymerization displays a marked deceleration consistent with the prediction of the mechanism shown in Scheme 1. Similarly, since this mechanism depends on free-radical-induced decomposition of an easily reduced diaryliodonium salt onium salt photoinitiator, the replacement by a triarylsulfonium salt with a higher reduction potential should result in a slowing of the rate. Figure 7 also shows the polymerization of **MCEP** using (4-decyloxyphenyl)diphenylsulfonium hexafluoroantimonate (**SOC10**) as a photoinitiator. While the structure of this photoinitiator closely resembles that of **IOC11**, and its quantum yield is similar, the reduction potential of **SOC10** is considerably higher.[23−25] As a result, it is not easily reduced by free-radical species and consequently

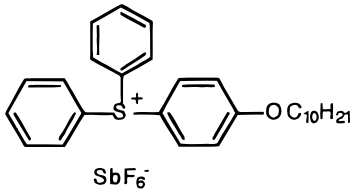

SOC10

does not undergo free-radical-induced decomposition reactions. As noted in Figure 8, the rate of epoxide polymerization of **MCEP** is greatly reduced when **IOC11** is replaced with **SOC10**. These two results are consistent with the mechanism proposed in Scheme 2.

The mechanism shown in Scheme 2 further leads to the prediction that acceleration of an epoxide polymerization should take place whether the 1-propenyl ether and epoxide groups are present in the same molecule or not. Verification of this prediction has already been demonstrated in the simultaneous polymerizations of equimolar amounts of 1-propenyl ethers and epoxides as noted in Figures 2 and 5. Additional studies were conducted that further confirm this hypothesis and will be reported in detail in a subsequent publication.

As an additional consequence of the consideration of Scheme 2, it may be anticipated that monomers such as **CEA**, **MCEA**, and **NEA** in which the allylic methylene protons may be easily abstracted by virtue of the resonance stabilization of the resulting allylic free radical should also exhibit an acceleration of the rate of epoxide ring-opening polymerization. This mechanism is depicted in Scheme 3 for **CEA**.

The allyl free radical formed in eq 20 can react further (eq 21) by a redox reaction with the diaryliodonium salt to give the resonance-stabilized allylic carbocation shown and a diaryliodine free radical. Rapid decomposition of the diaryliodine free radical (eq 22) gives an aryl iodide and simultaneously regenerates the aryl free radical completing the cycle. To detemine whether the mechanism shown in Scheme 3 is operative, it was first necessary to demonstrate whether epoxide ring-opening polymerization was really accelerated as a result of the presence of the allyl group in compounds such as **MCEA**. For this reason, we prepared **MCEPr** as a model compound. **MCEPr** contains the same number of carbon atoms as **MCEA**, and while it does bear labile protons on the carbons adjacent to the ether oxygen, these hydrogen atoms are not as easily abstracted as the allylic methylene protons in **MCEA**. A direct

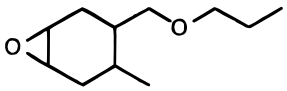

MCEPr

comparison of the rates of epoxide ring-opening polymerization of **MCEA** and **MCEPr** is shown in Figure 9. It may be readily seen from the RTIR curves that, as predicted, the photopolymerization of **MCEA** is considerably more rapid than that of **MCEPr**. We attribute this to the greater ability of the allyl group to stabilize both free-radical and cationic species and thus to support the presence of a free-radical-induced chain decomposition of the diaryliodonium salt photoinitiator. Similarly, the rate of epoxide ring-opening polymerization of **MCEP** is markedly faster than that of either **MCEA** or **MCEPr**, reflecting the greater efficiency of

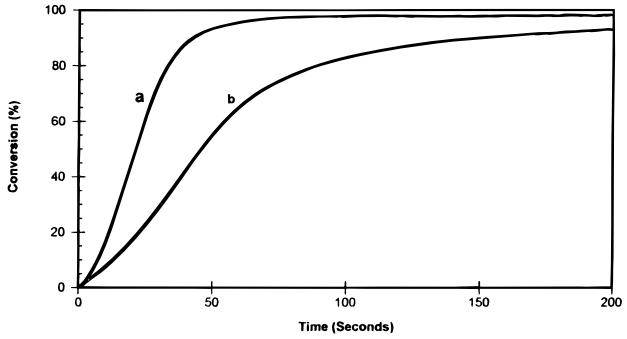

Figure 9. Comparison of the epoxide ring-opening photopolymerizations of **MCEA** (a) and **MCEPr** (b).

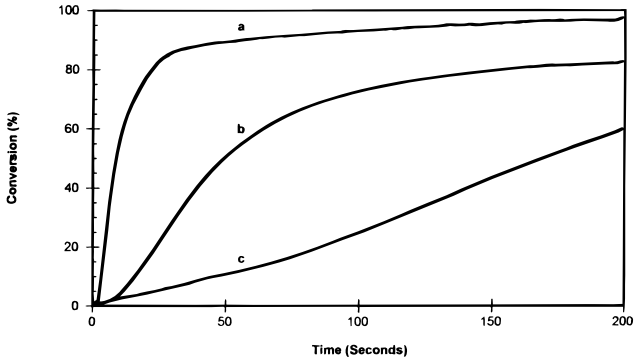

Figure 10. Comparison of the epoxide ring-opening photopolymerization of **MCEA** (a) alone, (b) in the presence of 4% nitrobenzene as a free-radical retarder, and (c) using **SOC10** as photoinitiator.

Scheme 3

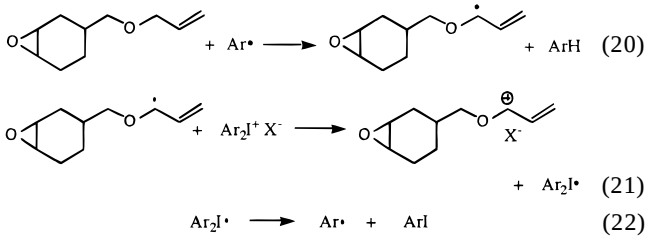

the mechanism shown in Scheme 2 in the acceleration of the epoxide polymerization.

As a further test for the validity of the mechanism shown in Scheme 3, we conducted a study of the photopolymerization of **MCEA** alone, in the presence of the retarder, nitrobenzene, and also using **SOC10** to replace **IOC11**. The results are shown in Figure 10. Considerable deceleration of the epoxide polymerization takes place with the inclusion of 4% nitrobenzene which is due to partial suppression of the free-radical-induced chain photoinitiator decomposition. An even greater deceleration of the polymerization rate is obtained when this process is entirely suppressed by replacement of the diaryliodonium salt with a triarylsulfonium salt photoinitiator which cannot undergo free-radical-induced decomposition.

Thermal Properties of Hybrid Monomers. The thermal properties of the three polymers prepared by the cationic photoinitiated polymerizations of **CEP**, **MCEP**, and **NEP** are given in Table 2. The glass transition temperatures (T_g's) as measured by DSC are quite high for these polymers. This could be due to several contributing factors. First, as noted earlier, polymerization of these monomers results in the formation of essentially a cross-linked polyethers containing stiff cycloaliphatic groups. The T_g of such polymers would be expected to be inherently high. Second, the polymerizations of the monomers are rapid and highly exothermic. Thus, despite the fact that the photopolymerizations were conducted at 25 °C, the actual temperature of the samples during polymerization are much higher to autoacceleration effects. This allows the T_g to rise during polymerization well above room temperature. In addition, the polymerizations were not terminated. As a result, during DSC measurements at a slow heating rate (5 °C/min), additional cationic polymerization can occur, resulting in a further elevation of the T_g. The polymers were also characterized by thermogravimetric analysis (TGA) in air at a heating rate of 20 °C/min. Preparation of the samples was found to be an important factor in the determination of the temperature at which 10% weight loss occurs. When the sample was prepared from powder samples prepared by pulverizing photopolymerized films of the polymers, comparatively low values of the thermal stability were obtained. However, when the photopolymerizations were carried out in the sample pans and then the TGA scans run, much higher results were obtained. Hence, the oxidative thermal stability results are highly dependent on the surface area of the sample. The results for the polymer derived from **NEP** show that this polymer is not very thermally stable. The reason for the low thermal performance of this polymer is not known at this time.

Table 2. Thermal Properties of Photocured Hybrid Monomers

polymer	T_g[a] (°C)	10% wt loss[b] film (°C)	10% wt loss[b] powder (°C)
CEP	176	464	332
MCEP	174	445	280
NEP	141	218	–

[a] Measured at 5 °C/min in air. [b] Measured at 20 °C/min in air.

Conclusions

Three hybrid monomers that incorporate both cycloaliphatic epoxy and 1-propenyl ether groups have been prepared in very good yields by simple, straightforward synthetic methods using inexpensive and readily available starting materials. The photoinitiated cationic polymerizations of these new monomers were followed using real-time infrared spectroscopy. It was observed that, contrary to expectation, the cationic ring-opening polymerization of the epoxide groups proceeded at higher rates than the vinyl polymerization of the 1-propenyl ether groups. With the aid of model compounds, it could be shown that rapid crossover from 1-propenyl ether polymerization to epoxide polymerization takes place which results in suppression of the 1-propenyl ether polymerization relative to the epoxide ring-opening polymerization. The apparent rate acceleration was shown to be due to the photoinduced free-radical decomposition of the photoinitiator which provides an increased rate of generation of initiating species. Similar enhancement of the rate of epoxide ring-opening polymerization of monomers bearing allyl ether groups was also demonstrated. These new, low-viscosity, high-reactivity monomers have many potential practical applications involving UV curing. In addition, this work also suggests alternative methods by which photoin-

duced cationic polymerizations of epoxides may be accelerated through rational structural design of monomers. We will report the results of logical extensions of the work presented here in future publications.

References and Notes

(1) Crivello, J. V.; Varlemann, U. *J. Polym. Sci., Polym. Chem. Ed.* **1995**, *33* (14), 2473.
(2) Crivello, J. V.; Narayan, R. *Macromolecules* **1996**, *29* (1), 433.
(3) Crivello, J. V.; Yoo, T. *J. Macromol. Sci., Pure Appl. Chem.* **1996**, *A33* (6), 717.
(4) Crivello, J. V.; Löhden, G. *J. Polym. Sci., Polym. Chem. Ed.* **1996**, *34* (10), 2051.
(5) Crivello, J. V. In *Developments in Polymer Photochemistry-2*; Allen, N. S., Ed.; Appl. Sciences Pub.: London, 1981; Chapter 1.
(6) Crivello, J. V.; Jo, K. D. *Polym. Mater. Sci. Eng. Prepr.* **1992**, *67*, 248.
(7) Crivello, J. V.; Bi, D. *J. Polym. Sci., Polym. Chem. Ed.* **1993**, *13* (12), 3109.
(8) Crivello, J. V.; Kim, W.-G. *J. Polym. Sci., Polym. Chem. Ed.* **1994**, *32* (9), 1639.
(9) Crivello, J. V.; Lee, J. L. *J. Polym. Sci., Polym Chem. Ed.* **1989**, *27*, 3951.
(10) Akhtar, S. R.; Crivello, J. V.; Lee, J. L. *J. Org. Chem.* **1990**, *55*, 4222.
(11) Doyle, M. P.; DeBruyn, D. J.; Kooistra, D. A. *J. Am. Chem. Soc.* **1972**, *10*, 3659.
(12) Crivello, J. V.; Jo, K. D. *J. Polym. Sci., Polym. Chem. Ed.* **1993**, *31* (6), 1473.
(13) Prosser, T. J. *J. Am. Chem. Soc.* **1961**, *83*, 1701.
(14) Kesslin, G.; Orlando, C. M. *J. Org. Chem.* **1966**, *31*, 2682.
(15) Crivello, J. V. *Makromol. Chem. Macromol. Symp.* **1988**, *13/14*, 145.
(16) Dektar, J. L.; Hacker, N. P. *J. Org. Chem.* **1990**, *55*, 639.
(17) Dektar, J. L.; Hacker, N. P. *J. Org. Chem.* **1991**, *56*, 1838.
(18) Decker, C.; Moussa, K. *J. Polym. Sci., Part A: Polym. Chem.* **1990**, *28*, 3429.
(19) Crivello, J. V.; Liu, S. S. *J. Polym. Sci., Part A: Polym. Chem.* **1998**, *36* (7), 1179.
(20) Crivello, J. V.; Narayan, R. *Macromolecules* **1996**, *29* (1), 439.
(21) Crivello, J. V.; Bratslavsky, S. A. *J. Polym. Sci., Polym. Chem. Ed.* **1994**, *32*, 2755.
(22) Crivello, J. V.; Fan M.; Bi, D. *J. Appl. Polym. Sci.* **1992**, *44*, 9.
(23) Grimshaw, J. In *The Chemistry of the Sulfonium Group*; Stirling, C. J. M., Patai, S., Eds.; John Wiley & Sons Ltd.: London, 1981; p 141.
(24) Pappas, S. P.; Gatechair L. R.; Jilek, J. H. *J. Polym Sci., Polym. Chem. Ed.* **1984**, *22*, 77.
(25) Kunze, A.; Müller, U.; Tittes, K.; Fouassier, J.-P.; Morlet-Savary, F. *J. Photochem. Photobiol., A: Chem.* **1997**, *110*, 115.

MA981078R